Film Fabrication of Perovskites and their Derivatives for Photovoltaic Applications via Chemical Vapor Deposition

*Mingyue Wang, Claire J. Carmalt**

Department of Chemistry, University College London, 20 Gordon Street, London, WC1H 0AJ, UK.

KEYWORDS: perovskite solar cells, chemical vapor deposition, scalability, photovoltaic, thin films

ABSTRACT:

In recent decades, metal halide perovskites have attracted much attention after showing great potential in photovoltaic (PV) applications. With the rapid progress of perovskites, various thin film fabrication methods have been studied intensively. However, in order to obtain perovskite films with the desired morphologies and properties and achieve large-scale manufacture, a film deposition method with controllability, cost efficiency, scalability and uniformity is required. Chemical vapor deposition (CVD) stands out among the various deposition methods due to its unique advantages. In this review, perovskite films for PV applications deposited by diverse

CVD methods are discussed, and a summary of the development and investigation of CVD processes utilized is provided.

INTRODUCTION

The investigation of renewable energy sources, especially solar energy, is increasingly popular due to current environmental problems and resource shortage. As an effective device to utilize solar energy, the perovskite solar cell (PSC) attracted much interest, because it is not only low-cost, but also highly effective. Since 2009, when the first perovskite film in the solar cell was fabricated by one-step spin-coating,[1] the perovskite field has flourished for more than one decade and keeps moving toward higher efficiencies and more facile fabrication methods. The state-of-the-art perovskite solar cell has reached a power conversion efficiency (PCE) of 25.6%, comparable to that of crystalline silicon solar cells.[2]

One feature of perovskites that makes them stand out from all semiconducting materials with excellent performance is their fabricability. Compared with other candidates, perovskite films in PV applications could be deposited through various cost-effective methods, including solution processes[3–8] and vapor processes.[9–11] However, perovskite thin films are typically deposited by spin-coating. While this method has short deposition process times, allowing for rapid reiteration and optimization, it yields films with poor uniformity over large areas, and the production is often limited to the use of a glovebox.[4,5] These problems all limit the mass production of perovskite films. In addition to spin-coating, various methods have also been developed for perovskite film deposition. For solution processes such as spray coating,[6] inkjet printing[7] and slot-die coating,[8] although they have been utilized on large-scale substrates, excessive variables in the coating process such as droplet size, substrate wettability and solvent boiling point means that formation of high quality films is challenging.[12,13] Solvent-free techniques such as thermal

evaporation[10] and flash evaporation[11] can produce high quality and pin-hole free films with large crystallites due to the slow film growth rate. However, the demand of high vacuum or high temperature increases the cost, and the number of suitable precursors is limited due to the requirement of thermal stability. Consequently, a simple, scalable and low-cost method to produce thin films of perovskite or perovskite-derived materials is required and chemical vapor deposition (CVD) could meet these demands.

CVD is a film deposition method involving a process containing a series of chemical reactions in the vapor phase. Due to its reliability, scalability and low cost, CVD has been industrially utilized in many optoelectrical fields, especially glass coating and semiconductors.[13] Based on the kind of energy to drive the chemical reaction used in the process, CVD can be classified as thermal CVD, photon CVD, laser CVD, plasma-enhanced CVD and pulsed CVD.[14] Considering the difference in vapor characteristics and operation processes, CVD can also adopt a range of variants, such as in low-pressure CVD (LPCVD),[15] metal-organic CVD (MOCVD),[16] and aerosol-assisted CVD (AACVD).[17] The thermal tubular CVD is still the most popular setup in both research laboratories and industries with numerous variants. The tubular reactor chamber allows for straightforward and suitable setups for desired film depositions. Normally, the quartz tube for CVD is surrounded by a heating furnace for controllable temperatures, which is called a hot-wall CVD. In some cases, the heating part could also be a heating 'table' inside the tube, which is then cold-wall CVD. A carrier gas flow, such as nitrogen or argon, goes into the tube from the inlet for the transport of precursors, although in LPCVD a vacuum would be utilized. The fundamental mechanism behind CVD involves the following steps: (1) Transport of precursors in the vapor phase to the reaction chamber; (2) Chemical reactions for the formation of intermediate species and by-products; (3) Transport of intermediate species to the substrates;

(4) Physical or chemical adsorption of reactants onto the substrate; (5) Heterogeneous reactions including diffusion, nucleation and growth leading to the target solid phase film formation on the substrate surface; (6) Desorption of by-products; (7) Removal of by-products and unreacted precursors away from the chamber.[14] As a result, CVD is an interdisciplinary process. Any one of the parameters such as temperature, flow rate and types of precursors could influence the final film deposited. At the same time, thermal tubular CVD is highly repeatable for the optimized film if the above parameters are controlled.

In 2014, CVD was first used to prepare perovskite materials for PV applications,[18–20] as a low-cost and high throughput method to produce PSCs on a larger scale. The CVD process allows for batch fabrication, which is helpful for sample-to-sample uniformity. In addition, the self-limiting nature of perovskite films deposited by CVD could improve batch-to-batch reproducibility.[21] The ease of controlling reaction temperatures, pressures and atmosphere in a tubular chamber soon made CVD attractive in the perovskite field. In addition, unlike common solution-based methods, the intercalating reaction rate of the film could be reduced in the vapor phase CVD process and the crystallization process could also be precisely controlled, which is beneficial to the formation of uniform and smooth films.[19,22,23] Diverse tubular CVD has been applied in thin film deposition of perovskites and their derivatives in PSCs.

At present, lead-based perovskites are the most studied kind of materials due to their outstanding performance. However, the toxicity and instability of lead are also nonnegligible. Therefore, many metal elements have been investigated for lead-free perovskite-like materials, and several metals, such as tin and bismuth, stood out among all candidates due to their low toxicity, ambient stability, and potential performance in PV devices. In recent years, several reviews containing CVD of perovskite films have been reported, which have focused on lead-

based perovskites.[12,13,24–26] This review will systemically summarize CVD of not only lead halide perovskites, but the film fabrication of lead-free derivatives by CVD will also be discussed. At the same time, a comparison and summary of the various films will be provided.

HYBRID CHEMICAL VAPOR DEPOSITION (HCVD)

HCVD is a potential method for the scale up of perovskite film deposition for PV applications. A complete HCVD process contains a metal halide film deposition through thermal evaporation or solution-based techniques and sequential perovskite conversion in the reactor under organic or inorganic halide vapor. Normally, a multi-zone furnace with flexible control of carrier gas, temperature and pressure is used in HCVD.

Thermal evaporation/CVD. HCVD was first utilized to deposit methylammonium lead iodide ($MAPbI_3$) film by Leyden et al. in 2014 and PSCs were demonstrated with efficiencies of 11.8%.[19] These devices were stored in dry N_2 and were stable up to 1100 h. A two-step process was carried out for the deposition, where a $PbCl_2$ film was first deposited on the substrate by high-vacuum thermal evaporation to provide a more uniform morphology than achieved with PbI_2, followed by a CVD deposition of methylammonium iodide (MAI). As shown in Figure 1a, in the HCVD process, the MAI powder and substrates were positioned in two zones with different temperatures of 185 ˚C and 130 ˚C, respectively. Finally, smooth $MAPbI_3$ films with thickness of 300 nm and grain size of ~ 0.6 μm were obtained. The thickness of the perovskite films was found to be determined by the $PbCl_2$ film, which would influence the device performance. In addition, substrates that were post-annealed in air led to a better device performance than those annealed in N_2 (Figure 1b).

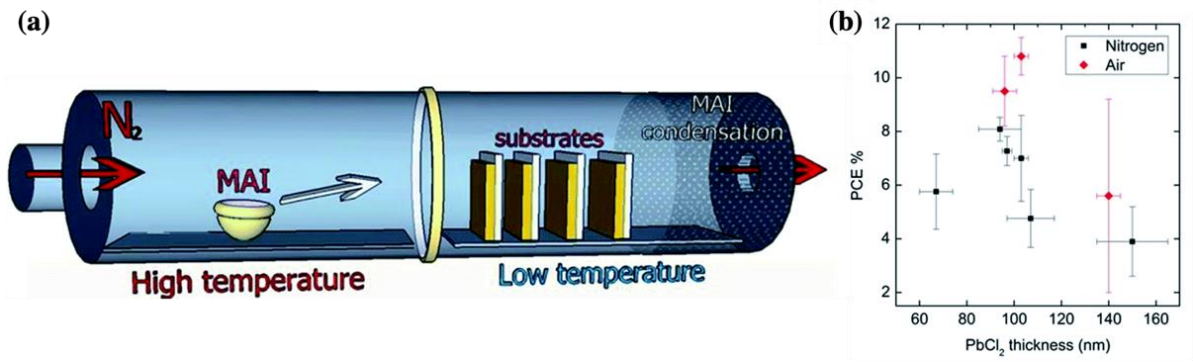

Figure 1. (a) Schematic illustration of the HCVD equipment with two temperature zones. (b) Scatter plot of average efficiencies of solar cells at different PbI_2 layer thicknesses and post-annealed atmospheres. Reproduced from ref. 19 with permission from the Royal Society of Chemistry. Licensed under a Creative Commons Attribution 3.0 International License (https://creativecommons.org/licenses/by/3.0/).

In another report by the same group, stable gamma-phase formamidinium lead iodide ($FAPbI_3$) films were fabricated using the same method.[21] Due to the presence of the FA cation, both the efficiencies and stability of the PSCs were improved significantly. Devices with the highest efficiencies of 14.2% and stability of 155 days were obtained. In this work, the performance and stability of PSCs were optimized through adjusting the formamidinium iodide (FAI) saturation and chlorine concentration in the films.

Leyden et al. further refined and scaled up the above deposition process, achieving the fabrication of PSCs based on $MAPbI_3$ (15.6%, 0.09 cm^2) and $FAPbI_3$ (9.5%, 8.8 cm^2; 9.0%, 12 cm^2).[27] A comparison between solution ($MAPbI_3$) and CVD ($FAPbI_3$) process cells determined that although PCEs of large-area PSCs *via* spin-coating were higher than those of CVD cells, due to overheating, the steady state power of solution processed cells declined rapidly with increasing active areas, which did not happen to CVD produced cells. This work suggested the potential scale-up of HCVD for perovskite film fabrication.

With the trend of mixing organic, inorganic cations and/or halides in perovskites for better morphologies, stability and tunable optoelectrical properties, the complexity of the material component was increased through more complicated HCVD process.[28,29] The deposition of Sn-rich $MASn_xPb_{1-x}I_3$ ($0<x<1$) films with large grain size over 5 μm from a solvent-free process was reported by Tavakoli et al., where a novel alloy technique was utilized.[28] A binary alloy precursor was selected to obtain the target perovskite with controlled composition and morphology. Lead and tin metals were deposited separately through thermal evaporation, and then MAI reacted with the alloy film in a tubular CVD chamber. Final PSCs based on these high-quality films yielded a PCE of 14.04%, which was comparable with pure Pb PSCs but with a much higher stability than pure Sn PSCs.

Lead perovskites films with binary cations and halides in the structure, such as $Cs_{0.1}FA_{0.9}PbI_{2.9}Br_{0.1}$, could also be prepared *via* HCVD.[29] The perovskite film with large grains and a smooth surface was obtained, and the film thickness was around 400 nm (Figure 2a,b). More importantly, the huge potential of HCVD in industrialized production was further demonstrated by as-obtained PSCs with a designed area of 91.8 cm^2 approaching 10% efficiency (Figure 2c, d). The remarkable performance and area of devices was comparable with those of films fabricated by solution-based methods such as slot die coating, and the utilization of toxic solvents was avoided at the same time.[30] The geometric fill factor (>90%) of modules in this work was much higher than other similar materials-based PSCs even with smaller areas.[31,32] Furthermore, PSCs' absolute efficiency decay was close to that of other scale-up commercialized PV devices (Figure 2e).

In addition to traditional tubular CVD reactor, a vapor transport deposition system featuring a showerhead was used in HCVD as well (Figure 2f).[33] This setup physically dissociates the

organic vapor evaporation zone from the deposition chamber, avoiding the complex control of the organic sublimation. The transport of MAI vapor through a showerhead could also ensure a spatially homogeneous conversion of PbI_2 to $MAPbI_3$, and homogeneous perovskite layers were deposited on textured silicon substrates (Figure 2g).

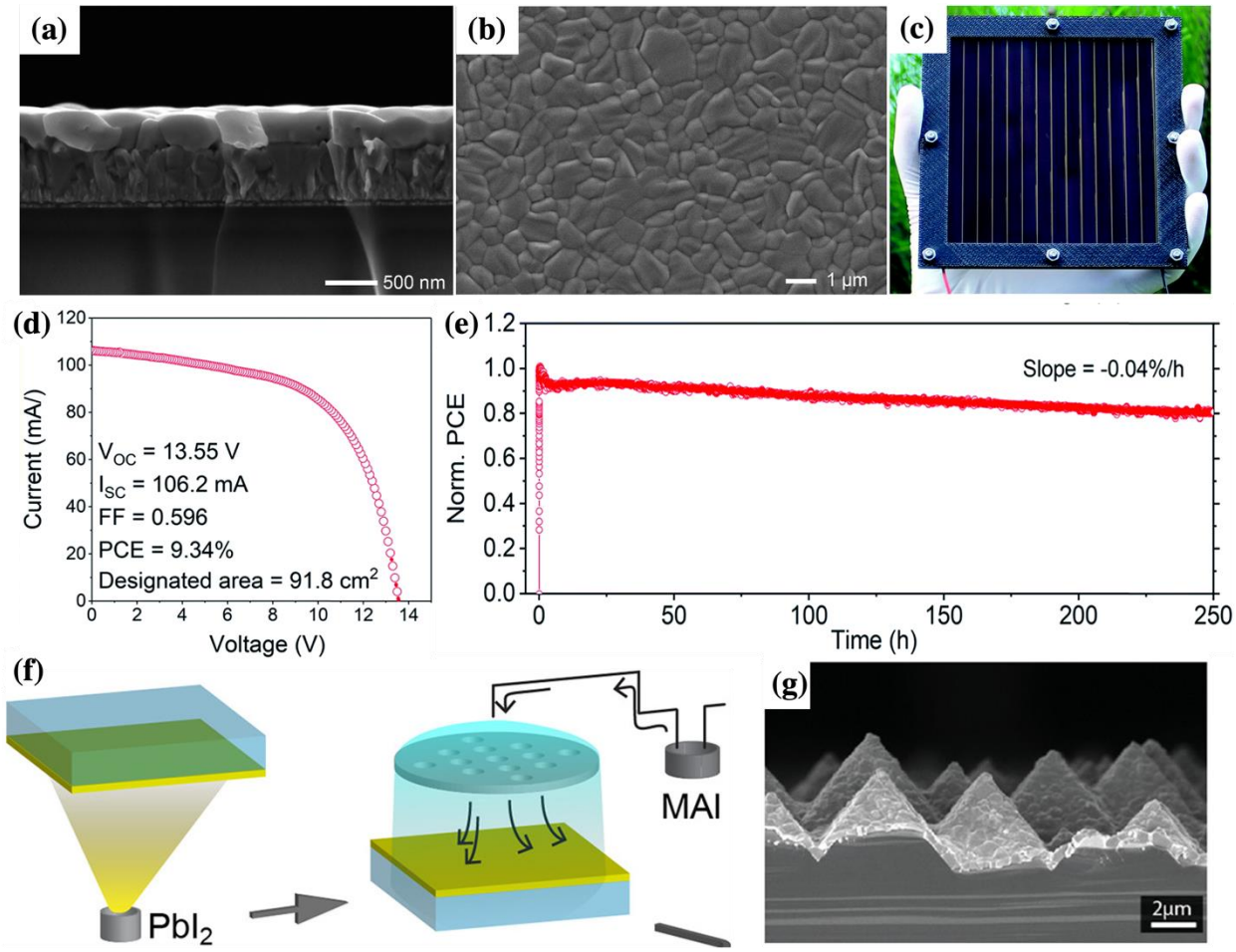

Figure 2. (a) Cross-sectional and (b) planar SEM images of the $Cs_{0.1}FA_{0.9}PbI_{2.9}Br_{0.1}$ film. (c) Optical image and (d) J–V curve of the 10 cm × 10 cm HCVD $Cs_{0.1}FA_{0.9}PbI_{2.9}Br_{0.1}$ based solar module. (e) Operational stability of the HCVD solar module under one-sun illumination and steady-state power output tracking. A burn-in loss of power output within the first ten hours with 90% of initial performance remaining, followed with a decay of the performance with a slope of -0.04%/h. Reproduced from ref. 29 with permission from the Royal Society of Chemistry.

Licensed under a Creative Commons Attribution-NonCommercial 3.0 International License (https://creativecommons.org/licenses/by-nc/3.0/). (f) Schematic illustration of the setup with showerhead. (g) Cross-sectional SEM image of the wafer. Reproduced with permission from ref. 34. Copyright 2021 American Chemical Society.

Although excellent PV devices have been successfully prepared through HCVD, the long deposition time of up to a few hours and obvious hysteresis would hinder the mass production of HCVD. Therefore, a rapid HCVD was developed to reduce the process time to less than 10 mins.[35] Both small cells (active area = 0.1 cm^2) and large modules (active areas = 22.4 cm^2) exhibited only slight hysteresis with great performance and stability.

Spin coating/CVD. In addition to thermal evaporation, CVD could also be compatible with solution-based methods, such as spin-coating. As a simple and mature film deposition method, spin-coating is widely used in combination with CVD, which is advantageous as spin-coating is more cost-effective than energy consuming thermal evaporation. While it is difficult to obtain large scale films, higher PCEs are normally obtained for spin-coated films due to the larger grain size compared with thermal evaporation.[36,37] Yin et al. reported vapor-assisted deposited $MAPbI_3$ PSCs with 18.9% efficiency based on spin-coated mesoporous PbI_2 films (Figure 3a).[23] This is the highest reported PCE of a CVD-deposited perovskite film, even though still inferior to that of the state-of-the-art $MAPbI_3$ PSC *via* spin-coating (beyond 21%).[38] In contrast to the previous HCVD reports, perovskite films of high quality were fabricated under ambient atmosphere, even at high relative humidity of around 60%, and *in situ* annealing under MAI vapor was introduced for recrystallization. From cross-sectional and planar SEM images, it can be seen that uniform films with large grains and dense morphology were deposited (Figure 3b, c). As a result, the devices showed remarkable air stability and low hysteresis. In addition, it was demonstrated that

compared with dense PbI_2 films, mesoporous PbI_2 films with smaller grains could benefit the MAI vapor migration, leading to the formation of perovskite films dominated by large crystals (Figure 3d, e). Besides Pb-based materials, HCVD was also successfully employed to fabricate less-toxic and more stable lead-free materials, such as methylammonium bismuth iodide ($MA_3Bi_2I_9$).[39] The performance of devices based on MA treated spin-coated BiI_3 films was comparable with those of solution-processed cells.

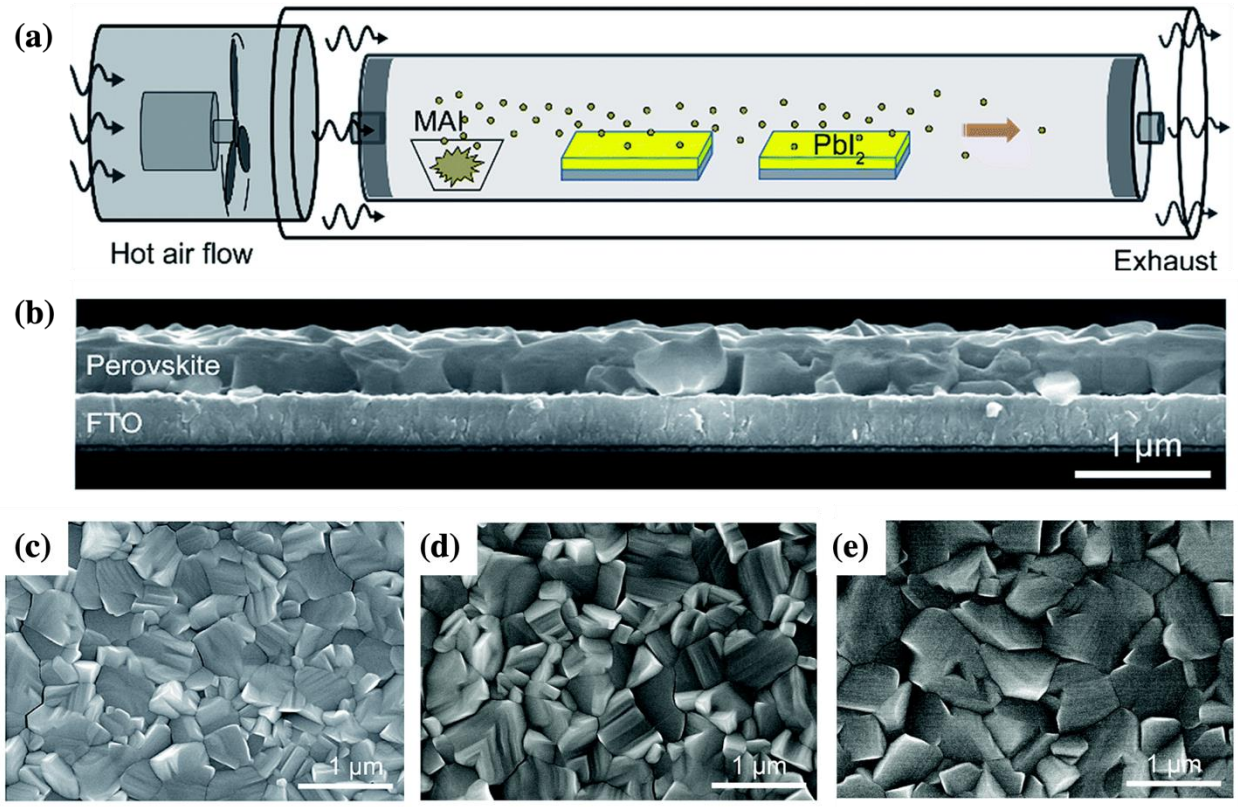

Figure 3. (a) Schematic illustration of the ambient atmosphere vapor-assisted deposition equipment. (b) Cross-sectional and (c) planar SEM images of the as-prepared perovskite film. $MAPbI_3$ films made by MAI vapor conversion of (d) dense PbI_2 films and (e) mesoporous PbI_2 film. Reproduced with permission from ref. 23. Copyright 2016 Royal Society of Chemistry.

The impact of CVD growth conditions on perovskite materials must be investigated to optimize film quality and device performance. The effect of carrier gas and postdeposition

cooling rate was studied by Ng et al..[40] It was found that a HCVD process in an N_2/O_2 (85%/15%) ambient with slow postdeposition rate could decrease the density of both shallow traps and deep levels in perovskites. Furthermore, a mesoscopic TiO_2 scaffold enhanced the device performance due to improved crystallization of the $MAPbI_3$ films and carrier transport properties of the whole device (Figure 4a, b). The same group performed low-frequency noise characterizations to determine that the $MAPbI_3$ films with higher crystallinity and lower defect density were fabricated by HCVD compared with films from the solution technique (Figure 4c, d), and oxygen annealing could passivate the films' defect states and improve the device stability. The highest PCE of the device based on the HCVD-grown film (16.9%) was improved significantly compared with the one prepared from the conventional solution method (9.9%).[41]

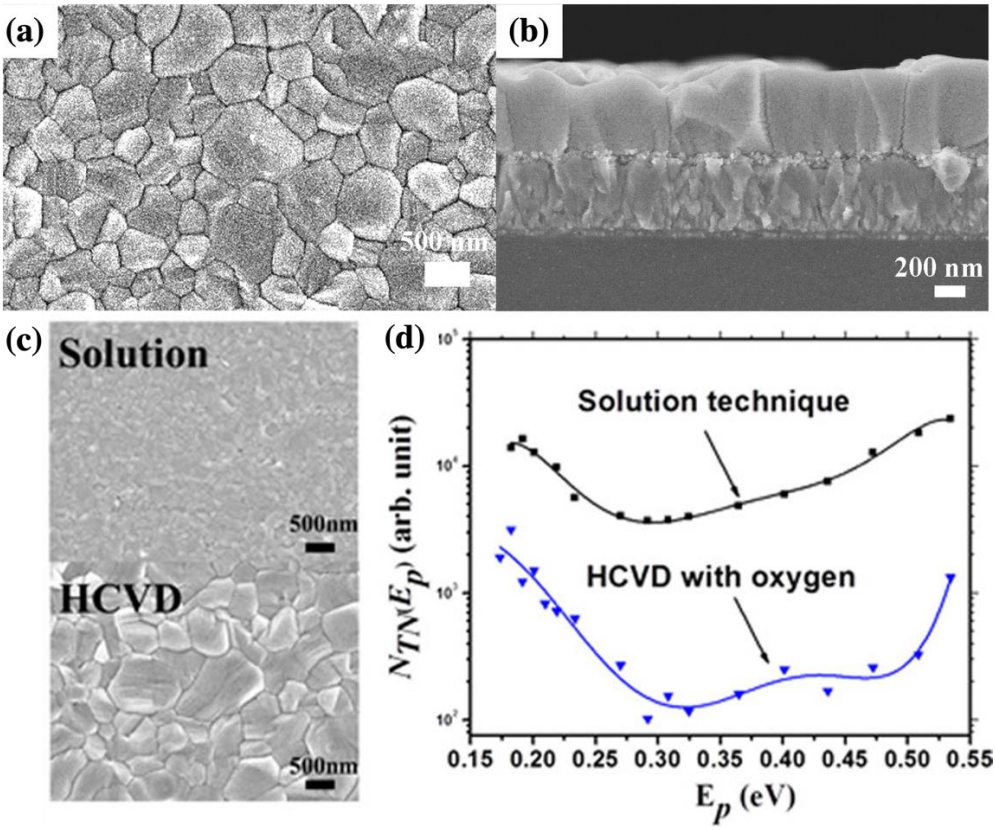

Figure 4. (a) Planar and (b) cross-sectional SEM images of the HCVD-grown $MAPbI_3$ film with slow cooling (0.7 °C/min) on mesoscopic TiO_2. Reproduced with permission from ref. 40. Copyright 2016 American Chemical Society. (c) SEM images of $MAPbI_3$ films grown by solution and HCVD techniques. (d) Normalized trap density computed for two types of resistive structures as a function of energy. The variation of trap density as a function of the activation energy has impact on the properties of the low-frequency noise power spectral density. Reproduced with permission from ref. 41. Copyright 2018 American Chemical Society.

The combination of spin-coating and CVD result in an increase in the range of potential precursors that can be utilized. Not only limited to organic halides, gaseous methylamine (MA) and HI could be used directly as precursors for $MAPbI_3$ film deposition, leading to a lower required CVD deposition temperature than that of other HCVD process.[42] At the same time, MA has been shown to have a defect-healing effect on $MAPbI_3$ films caused by the formation of an intermediate $CH_3NH_3PbI_3 \cdot xCH_3NH_2$ liquid phase.[43]

Jiang et al. first proposed a combination of HCVD and cation exchange (CE) to deposit large-scale (12 cm^2) $Cs_{0.07}FA_{0.93}PbI_3$ films (Figure 5a).[31] The smoothness and device performance of the HCVD-CE films were improved significantly compared with the solution-process films (Figure 5b, c). As-fabricated PSCs showed a PCE of 14.6% and PCE loss/active area of 0.17%/cm^2. It was shown that the Cs^+ ratio in the film influenced the grain size, electron and hole injection between layers. Furthermore, the improved stability of $Cs_{0.07}FA_{0.93}PbI_3$ films was caused by the higher Cs^+ ratio at the surface than that in the bulk. It was noted that HCVD could not only be used in the reaction between metal halides and organic/inorganic halides, but also anion exchange of perovskite materials. Unlike HCVD followed by a cation exchange process, anion replacement in perovskites was achieved in HCVD. Luo et al. used a tubular CVD setup to

achieve a fast anion exchange from $CsPbI_3$ to $CsPbBr_3$ under a Br_2 atmosphere.[44] This work avoided complicated solution-based synthesis of all inorganic perovskite films and the solubility limitation of bromide anions in conventional solvents. After the anion exchange, the structural stability of the perovskites was enhanced greatly, and a high efficiency of 5.38% was obtained for relevant cells. Following this an extra MAI/MABr-assisted CVD process was added after the anion exchange by the same group to fabricate bandgap tunable $CsPb(I_xBr_{1-x})_3$ films.[45] As the amount of MAI increased, the bandgaps decreased, and the grain size increased while the stability of films deteriorated.

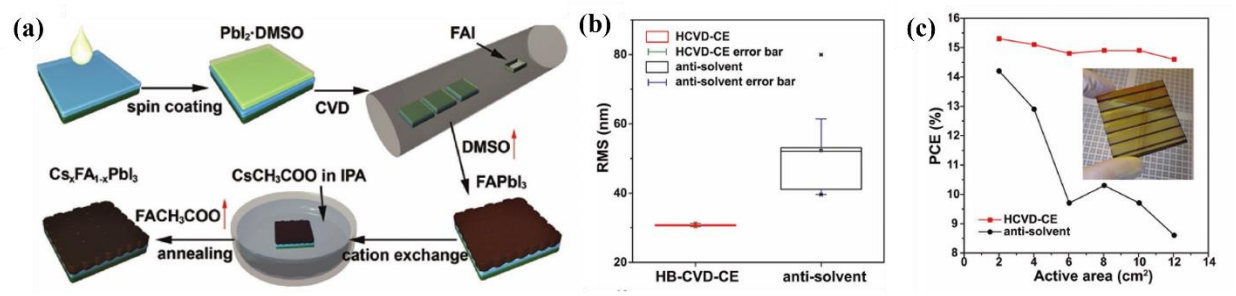

Figure 5. (a) Schematic illustration of the preparation of the mixed $Cs_xFA_{1-x}PbI_3$ perovskite films by the HCVD-CE method. (b) Surface roughness on the nine intentionally selected points of the 5 cm × 5 cm perovskite films. (c) PCE of the modules with different number of cells in series and photograph of a HCVD-CE prepared module. Reproduced with permission from ref. 31. Copyright 2017 Wiley-VCH.

Besides spin-coating, an up scalable perovskite deposition technology combining raster ultrasonic spray coating (RUS) and CVD was proposed (Figure 6a).[46] This novel method overcomes the coating size limitation of spin-coating (Figure 6b, c) and reduces Pb waste significantly during PbI_2 deposition (Figure 6e), increasing the potential of HCVD mass production and being more environmental friendly. Compared with spin-coating, this method

showed much lower substrate size dependence, and the perovskite module achieved a high module PCE of 14.7% on an active area of 12.0 cm^2 (Figure 6d).

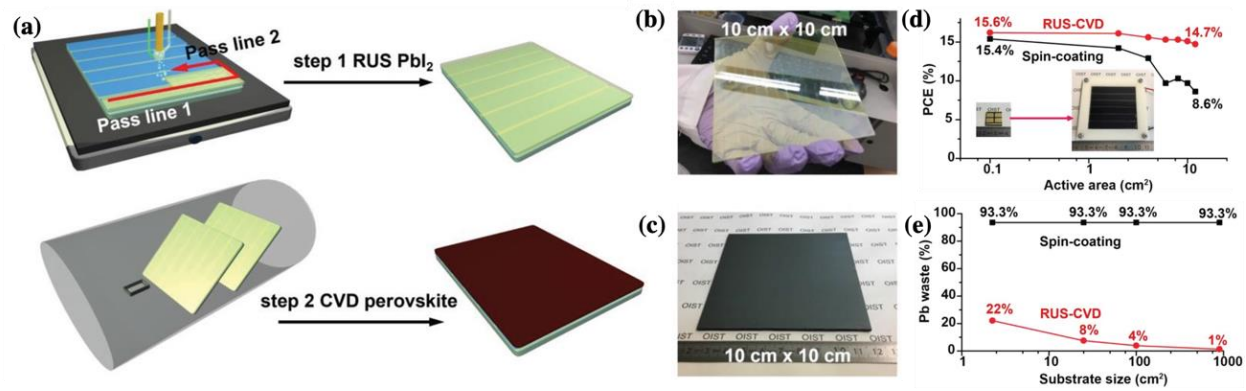

Figure 6. (a) Schematic illustration of the RUS–CVD technology. Photographs of (b) a RUS-coated PbI_2 film before annealing and (c) a CVD-converted $FAPbI_xBr_{3-x}$ film deposited on a 10 cm × 10 cm patterned fluorine doped tin oxide (FTO) substrate. (d) Solar cell and module performance as a function of active area. Spin-coating data are extracted from previous work.[31] (e) Lead waste during the perovskite deposition process as a function of substrate size. Reproduced with permission from ref. 46. Copyright 2019 Wiley-VCH.

LOW-PRESSURE CVD (LPCVD)

Conventional LPCVD. Despite its popularity, HCVD still has some disadvantages. In the HCVD process, a variety of intercalated parameters, which influence the film growth, are hard to adjust independently. LPCVD has been seen as a mature technology to deposit films on the industrial scale. Under a low-pressure environment (0.001 to 100 Torr), unwanted vapor phase reactions could be avoided and over-rapid intercalating reaction rate between metal and organic halides could be moderated, so that the uniformity and purity of the desired films are improved. In addition, the energy budget and yield of perovskite film deposition are improved for LPCVD.[47] Through combination with spin-coating, LPCVD was first introduced in PSC

preparation by Luo et al. (Figure 7a).[22] The prepared uniform $MAPbI_3$ films showed good crystallization and remarkable moisture resistance under laser illumination and high-temperature conditions. The as-obtained PSCs achieved an efficiency of 12.73% under open air with a high humidity above 60%. The main reason for these high-quality films was that in LPCVD, the long MAI molecular free path eliminated the gas concentration gradient, and the film could grow slowly layer-by-layer.

Shen et al. reported a different LPCVD with a single-temperature zone reactor to increase the material use ratio and large-scale capability (Figure 7b).[48] The crucial effect of reaction time and working pressure on the film formation was discussed. Large grain facets could be observed after 0.5 h, but the small grain prevailed over grain boundaries once the reaction time was up to 1 h (Figure 7c, d). Meanwhile, MAI vapor phase caused the decomposition or impurity formation of perovskites at high pressure. Based on the optimized $MAPbI_3$ films, PCEs of 15% and 6.22% were obtained respectively for small cells and large modules with active area of 8.4 cm^2. In addition, based on a mixed organic cation perovskite, the influence of carrier gas flow rate on physical and optoelectrical properties of the films was investigated in LPCVD process in another work.[49] A higher H_2 flow led to accelerated nucleation and grain growth, as well as more defects or contamination on the film surface.

The potential scalability of LPCVD for perovskite fabrication was also demonstrated. Luo et al. reported that uniform and pin hole-free $Cs_xFA_{1-x}PbI_{3-y}Br_y$ films were prepared from a method containing the thermal evaporation of CsBr and PbI_2 and LPCVD under FAI/FACl vapor.[32] It was shown that the morphology, stability and reproducibility of the final films were improved through adding FACl, due to the increased crystal growth rate (Figure 7e). In addition to PSCs with PCE as high as 17.29%, large sized 41.25 cm^2 PSC modules were also built up, exhibiting a

champion PCE of 12.24% (Figure 7f). While the highest PCE of $Cs_xFA_{1-x}PbI_{3-y}Br_y$-based devices has been achieved above 21%,[50] this efficiency is still remarkable for the device with such large active area.

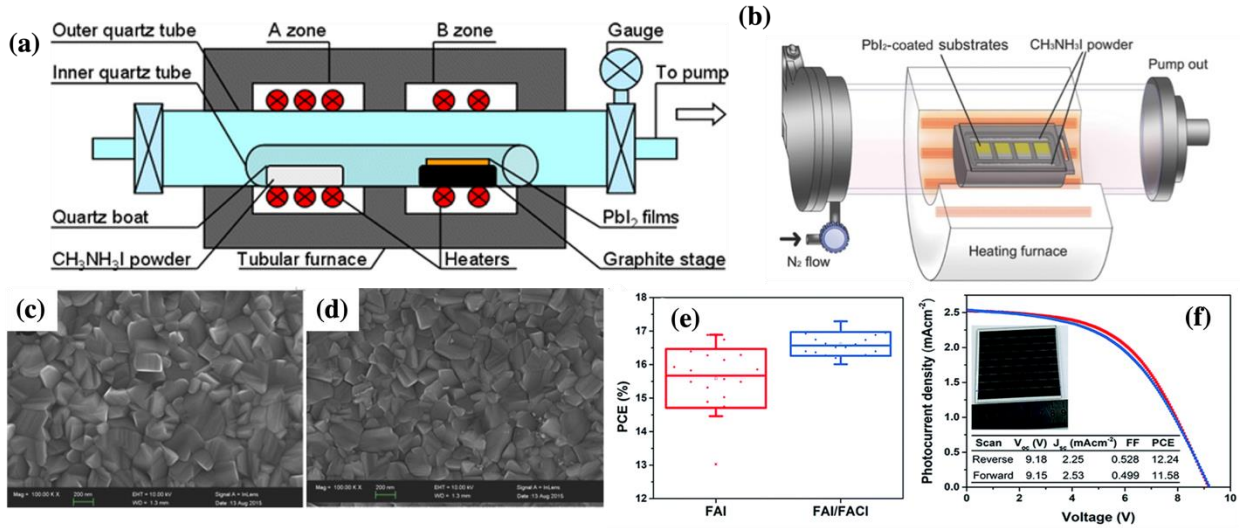

Figure 7. (a) LPCVD equipment with two-temperature zones. Reproduced with permission from ref. 22. Copyright 2015 American Chemical Society. (b) LPCVD equipment with single temperature zone. SEM images of $MAPbI_3$ films undergoing reaction times of (c) 0.5 h and (d) 1 h, Reproduced with permission from ref. 48. Copyright 2016 Wiley-VCH. (e) PCE value distributions of the device fabricated in FAI and FAI/FACl vapor. (f) J–V curves of PSC modules of size 8 × 8cm^2. Reproduced with permission from ref. 32. Copyright 2018 Royal Society of Chemistry.

As well as combining with spin-coating or thermal evaporation, LPCVD could also be utilized to prepare perovskite films solely through sequential deposition in one reactor.[51–54] As a result, the whole deposition process could be simplified further. $MAPbI_3$ films with large grain size of around 3.8 μm were obtained through two-step LPCVD, and the morphology of the final perovskite film was determined by the LPCVD-PbI_2 film.[51] Using more complex precursors or

adding more CVD steps, perovskite films with mixed metals or halides could be fabricated as well, such as Sn-doped and Cl-doped $MAPbI_3$.[52,54] It is worth noting that the thin films of lead-free materials, Cs_2SnI_6 and $MA_3Bi_2I_9$, were successfully synthesized by sequential LPCVD.[55–57]

Hybrid Physical Chemistry Deposition (HPCVD). For both aforementioned HCVD and LPCVD, a long-distance transport of the organic halides vapor is necessary, which affects the reproducibility of the fabrication process negatively. Therefore, a novel CVD setup derived from LPCVD was reported as hybrid physical CVD (HPCVD) in 2015.[58] Unlike HCVD and conventional LPCVD with multi-temperature zones and/or varied vacuum levels, perovskite films *via* HPCVD could be prepared in isothermal and well-controlled vacuum conditions. The precursor powder is placed below the substrate to decrease the transport distance (Figure 8) and because of the existence of two blocks, the gradient of the pressure in the tube, which typically diminishes from the inlet to outlet, was in a stable state. Consequently, vapor pressure could be modified simply through changing the configuration between precursors and substrates.[58] Peng et al. combined this refined LPCVD with the thermal evaporation of PbI_2 to deposit perovskite materials for PV applications.[58] $MAPbI_3$ solar cells prepared at an ultra-low temperature of 82 ˚C showed the highest PCE up to 14.7%. Later, through adding one more thermal evaporation step on the basis of HPCVD, Tong et al. demonstrated a precisely tunable stack sequence physical-chemical vapor deposition to prepare a CsBr-doped $FAPbI_3$ perovskite with high stability (Figure 8b).[59] This method featured a gradient bandgap profile to improve the PCE from 11.69% in pure $FAPbI_3$ to 18.22% in doped PSCs (Figure 8c).

In other HPCVD reports, optimized PbI_2 film *via* spin-coating was used as substrates,[60] and the relationship between spin-coating speed, precursor solution concentration, film quality and device performance was investigated.[61,62] In the solution process, it has been found that PbI_2

films with poor quality would lead to porous perovskite films with incomplete conversion.[63] Therefore, it is also important to avoid this risk in the CVD process with spin-coated PbI_2 substrates, and Luo et al. found that Cl introduction in the CVD process could repair defects in PbI_2 films.[64]

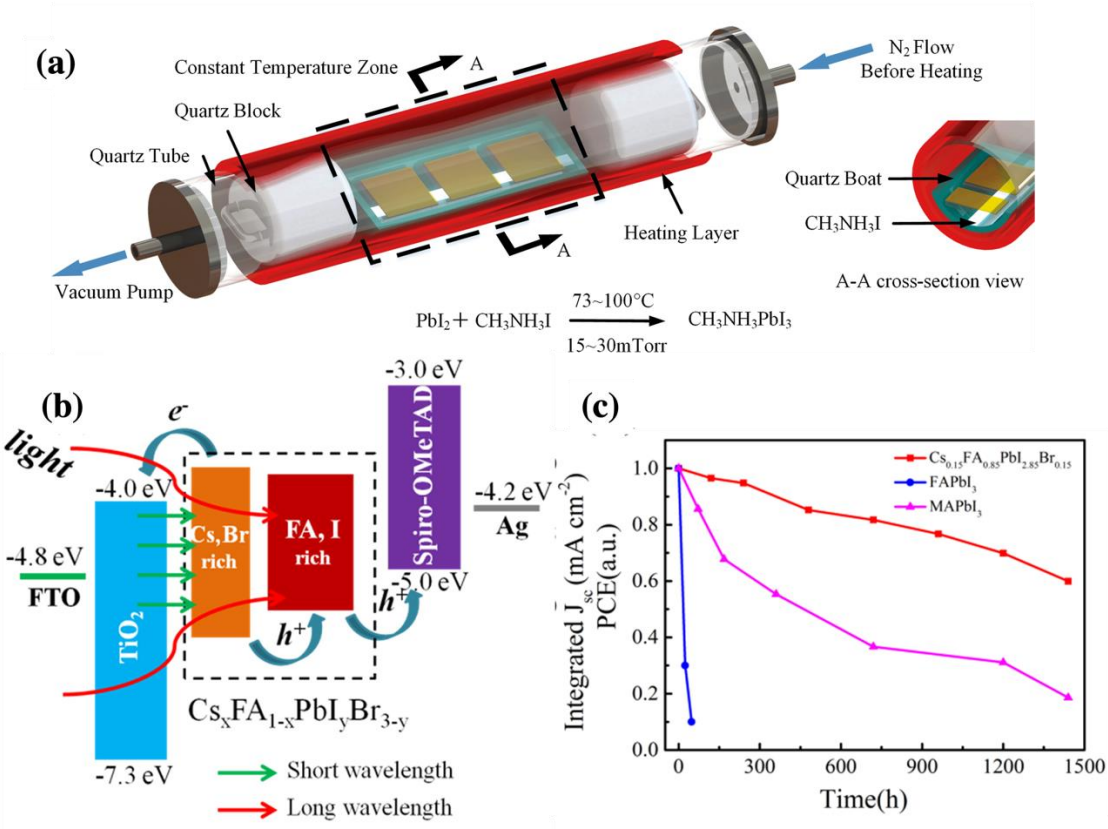

Figure 8. (a) Schematic illustration of a HPCVD method. Reproduced with permission from ref. 58. Copyright 2015 Royal Society of Chemistry. (b) Energy diagram of the PSCs via the stack sequence physical-chemical vapor deposition process. (c) Comparison of the stability of $MAPbI_3$, $FAPbI_3$ and CsBr-doped $FAPbI_3$ perovskite devices. Reproduced with permission from ref. 59. Copyright 2018 Elsevier.

Similar to HPCVD, an isothermal LPCVD tubular was utilized in a paper involving as-prepared $MAPbI_3$ films were stable up to 100 days in air.[65] The stability of the films was

enhanced by the synergistical effect of outstanding film purity, morphology and tight arrangement of crystallites. It is interesting that the highest PCE (15.15%) of cells was obtained after 30 days as a result of the formation of PbI_2 and self-healing of the defect state.

In-situ tubular CVD (ITCVD). In-situ tubular CVD (ITCVD) is also a kind of modified LPCVD. The intrinsic difference between HPCVD and ITCVD is the configuration of substrates and precursors in the reactor, which is "face-to-face" for ITCVD (Figure 9a) but "back-to-face" for HPCVD (Figure 8a). Luo et al. reported compact films produced through ITCVD, as shown in Figure 9b.[66] Interestingly, a roll-over phenomenon in J-V curves was first reported in PSCs (Figure 9c). Later, Liu et al. introduced NH_4Cl in ITCVD to reduce the reaction time and decrease the deposition temperature, which further reduced the energy consumption.[67] Moreover, the influence of PbI_2 deposition rate on films *via* PVD/CVD has been studied, proving that PbI_2 films with lower surface roughness and a higher degree of preferential growth orientation were deposited with higher rate, which was beneficial to form perovskite films with less residual PbI_2 in the ITCVD process.[68]

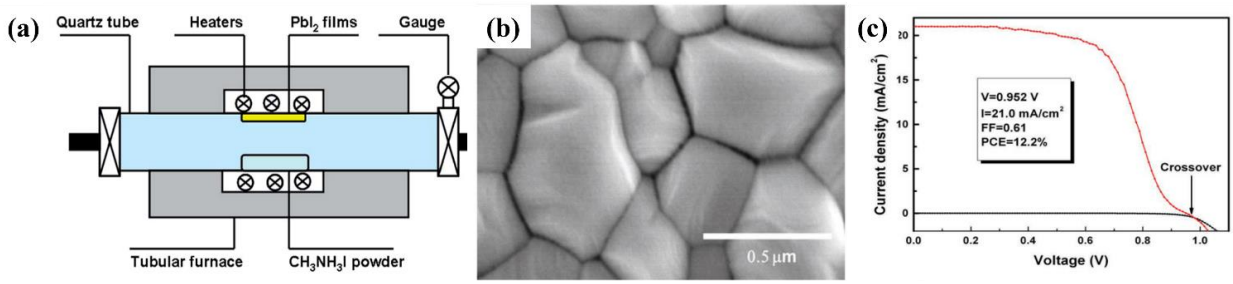

Figure 9. (a) Schematic illustration of ITCVD setup. (b) SEM image of thin film. (c) J–V curve of the PSC. Reproduced with permission from ref. 66. Copyright 2015 Royal Society of Chemistry.

In addition, a related method to ITCVD, close space vapor transport method, was presented by Li et al,[69] which is also a low-cost, high-throughput and scalable technology for semiconductor

fabrication. In this work, the large-area $MAPbI_3$-PSC had a PCE of 13.8% and great uniformity on a 3 cm × 3 cm substrate.

ONE-STEP CVD

Compared to multi-step methods, one-step CVD is a more facile process by eliminating other steps such as spin-coating and thermal evaporation. As a result, less deposition parameters need to be controlled in the process, which improves the reproducibility and cost effectiveness of the fabrication method.

The first investigation utilizing one-step tubular CVD was reported by Tavakoli et al.[70] Through the co-vaporizing of lead chloride or lead iodide and MAI placed in the high-temperature zone, $MAPbI_3$ and $MAPbI_{3-x}Cl_x$ films with large grain size, long carrier diffusion length and high coverage could be deposited in the low-temperature zone (Figure 10a). As-synthesized $MAPbI_{3-x}Cl_x$ films were used as the absorber layer in the planar solar cells with a PCE of 11.1%, and there is still potential room for device efficiency improvement. Hole-transport-material-free PSCs based on $MAPbI_3$ films *via* one-step CVD were also studied.[71] The effect of deposition parameters such as temperature, pressure and substrate on film morphology were also demonstrated in one-step CVD.[71,72] A kind of highly luminescent inorganic perovskite film, $CsPb_2Br_5$, was deposited by one-step CVD as well, and its properties was studied to prove the potential in PV applications.[73] Interestingly, thin films of lead-free materials were also successfully deposited *via* one-step CVD at ambient atmosphere or controlled pressure.[74,75] The novelty in the deposition process of $MA_3Bi_2I_9$ is the showerhead-based deposition tool for perovskites, which offered precise control options and paved the way for large-area production (Figure 10b).[75] Recently, it was first demonstrated that one-step CVD could also be utilized to

deposit millimeter-size $CsPbBr_3$ crystalline thin films with high phase purity, showing a promising preparation method suitable for PV applications (Figure 10c, d).[76]

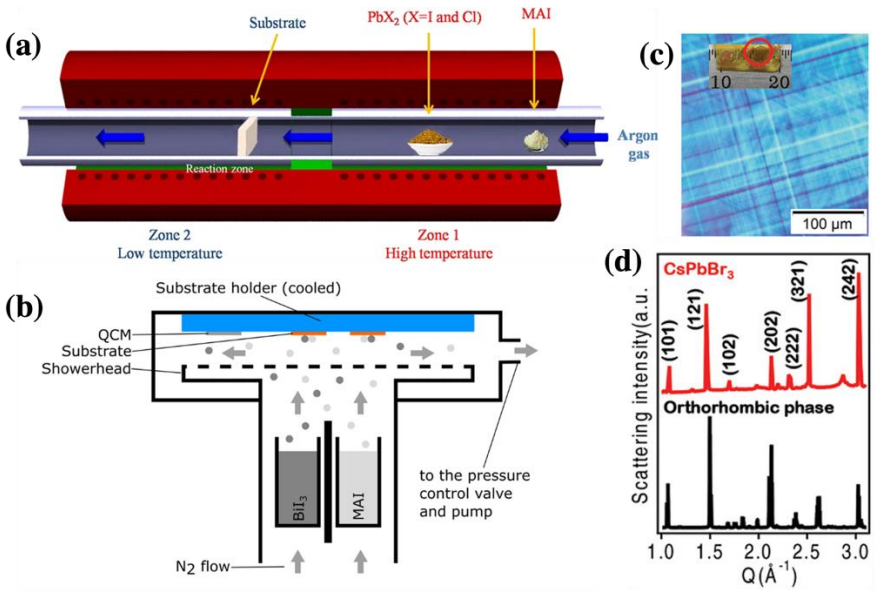

Figure 10. (a) One-step film fabrication using MAI and PbX_2 sources in a CVD furnace. Reproduced from ref. 70 with permission from Springer Nature. Licensed under a Creative Commons Attribution 4.0 International License (https://creativecommons.org/licenses/by/4.0/). (b) The showerhead-based deposition tool. Reproduced from ref. 75 with permission from Springer Nature. Licensed under a Creative Commons Attribution 4.0 International License (https://creativecommons.org/licenses/by/4.0/). (c) Polarized optical microscopy image for a single grain. The inset is the photograph of CVD grown $CsPbBr_3$ film with mm-scale grains. (d) The line-cut extracted from GIWAXS map (red) and simulated X-ray diffraction pattern (black) of orthorhombic phase $CsPbBr_3$. Reproduced with permission from ref. 76. Copyright 2021 Wiley-VCH.

AEROSOL-ASSISTED CVD (AACVD)

All CVD methods discussed in this review so far are solvent-free processes. In fact, solutions could also be utilized in CVD, such as with aerosol-assisted CVD (AACVD). As an emerging method with a large potential in industrial applications, AACVD has been widely used in the thin-film deposition of traditional functional materials, such as transparent conducting oxides and superhydrophobic materials.[77,78] Recently, semiconductor films of perovskites, bournonites and their derivatives deposited *via* AACVD have also been investigated as the absorber layer in solar cells.[20,79–82] AACVD combines the benefits of solution- and vapor-based deposition. There are basically two kinds of AACVD instruments, including hot-wall and cold-wall reactor (Figure 11). Through utilizing an ultrasonic humidifier, the mist of the precursor in a solution can be formed, followed by being transmitted into the heating reactor *via* a carrier gas flow. With the effect of high temperature, the film can be deposited after the evaporation of solvents and decomposition of precursors. The choice of precursors with high volatility is the main problem for traditional CVD. However, the mist form of precursors allows AACVD to remove this limitation, and simply require precursor solubility. This feature enlarges the varieties of suitable precursors in AACVD significantly.[83]

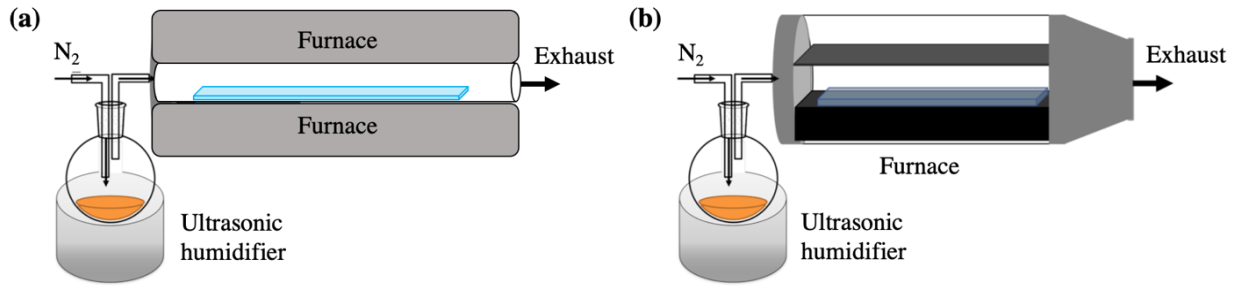

Figure 11. Schematic diagram of (a) hot-wall and (b) cold-wall AACVD instruments.

One-step AACVD. Different from solvent-free CVD, as precursors could react *in situ* in the solution, single-source precursor solutions are generally used in one-step AACVD, which is

more efficient and it is possible to reduce the deposition temperature required. In 2014, one-step AACVD was first utilized in the film deposition of $MAPbBr_3$ on glass at 250 ˚C, where the precursor solution in DMF was diluted with acetonitrile.[20] Later on, $MAPbI_3$ films were also deposited at 200 ˚C by AACVD.[79] However, these films were unstable, and slow decomposition happened under X-ray irradiation in XPS. In addition, a PbI_2-MAI-DMF intermediate complex was observed in the XRD patterns,[84] which was a common phenomenon for films deposited by AACVD due to the utilization of polar solvents with high boiling points.

Afterwards, the versatility of AACVD was further proved with various perovskites and related materials synthesized, such as $FAPbI_3$, Cs_2SnI_6 and phenethylammonium bismuth iodide ($PEA_3Bi_2I_9$).[80,82,85,86] In the case of $PEA_3Bi_2I_9$, three kinds of materials (glass, TiO_2 and FTO) were used as substrates to study their effects on the morphology and optoelectrical properties of the films.[82] It was shown in the SEM images that more compact, uniform and crystallized films were deposited on TiO_2 and FTO, demonstrating a positive effect of crystalline substrates on the film growth (Figure 12). Meanwhile, films of materials with mixed halides were reported by using more complex precursor solutions, including Cl incorporated $MAPbBr_3$, $CsPbBr_2I$ and bromine doped $MAPbI_3$.[87–89] Through changing the doping ratio, those films deposited by AACVD could be optically tuned.[87,89]

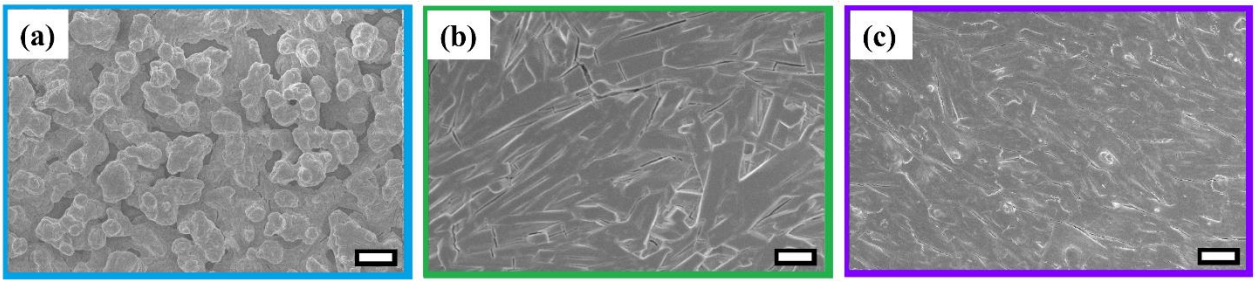

Figure 12. SEM images of $PEA_3Bi_2I_9$ on (a) float glass, (b) TiO2/glass and (c) FTO/glass substrates. Magnification for all images is x 1000 and scale bar represents 10 μm. Reproduced

from ref. 82 with permission from Wiley-VCH. Licensed under a Creative Commons Attribution 4.0 International License (https://creativecommons.org/licenses/by/4.0/).

In addition, additives in the precursor solutions were investigated to improve the film quality. For example, oleylamine, as a shape modifier, was chosen to be added into the precursor solution to modify the formation of $CsPbBr_2I$ microsquares.[88] Addition of HI was also found to reduce the number of macroscopic defects e.g., pinholes, iodine deficiency or the presence of impurities, and significantly influence the film properties (Figure 13a-d).[80]

The comparison between Cs_2SnI_6 and $MAPbI_3$ perovskite films deposited *via* AACVD at 130 °C and spin coating was investigated by Ke et al.. Larger grain sizes for AACVD grown films contributed to an improved stability (Figure 13e, f). They studied the film stability using near ambient pressure XPS, giving an insight into the degradation mechanism of perovskite films in humid air.[80,90] Unfortunately, until now, no complete PV devices has been built up successfully based on one-step AACVD perovskite films. The possible reason is the over-large thickness and pinholes of AACVD films.

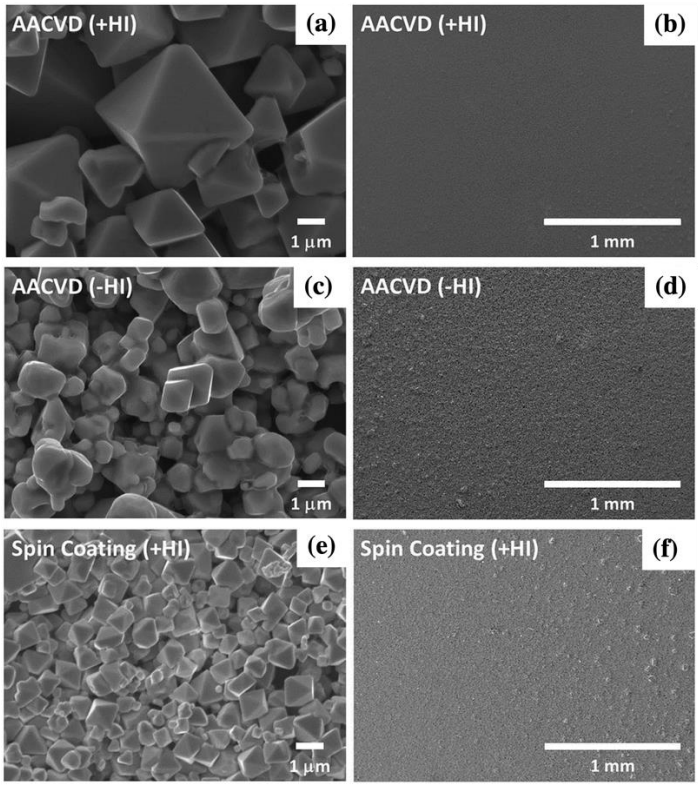

Figure 13. SEM images of Cs_2SnI_6 films (a), (b) AACVD (+HI)-processed film. (c), (d) AACVD (−HI)-grown film. (e), (f) spin-coated (+HI) film at higher and lower magnifications. Reproduced from ref. 80 with permission from the Royal Society of Chemistry. Licensed under a Creative Commons Attribution 3.0 International License (https://creativecommons.org/licenses/by/3.0/).

Multi-step AACVD. AACVD was developed from single step to two steps by Chen et al.[91] It was inferred that not densely packed perovskite coatings originated from the high deposition temperature in one-step process, which explained the poor morphology of $MAPbI_3$ films deposited by one-step AACVD.[79] While a small quantity of PbI_2 were not fully converted, compact and uniform films with grain size of 1-2 μm and film thickness of 1.5 μm were obtained. In this work, the temperature of the first deposition of PbI_2 was 70 ˚C, and the second deposition was at 220 ˚C.

Originating from the above two-step AACVD, a three-step AACVD with one more step to evaporate DMF in PbI_2 films was proposed.[92] As-prepared dense and uniform $MAPbI_3$ films with a thickness of 400 nm showed strong absorption and emission characteristics, but the films still lacked enough stability.

Compared with single-step AACVD, the thickness of perovskite films deposited *via* two- or three-step methods was significantly reduced, which is more desirable for the manufacture of effective devices. The first PV device based on the AACVD deposited absorber layer was fabricated by Ratnasingham et al.[93] Films were deposited *via* two-step AACVD (175 + 220 ºC) with lead acetate and MAI as precursors, and in both steps, methanol was the only solvent. Compared with common solvents used in perovskite fabrication like DMF, methanol has less toxicity, low surface tension and easy aerosolization. The obtained film had a good surface coverage, grain size of 1 μm and thickness around 1 μm, but the rough film surface had to be compensated with spray coated thick CuSCN as a hole transport layer in the device, which significantly limited the PCE (Figure 14). The PSC showed a relatively low PCE of 5.42%, as well as severe hysteresis due to non-ideal interfaces. Interestingly, AACVD was used in the post-deposition treatment for PSCs recently, which remarkably improved the efficiency and stability of devices.[94] This strategy was universally applicable to a wide range of PSC configurations and architectures.

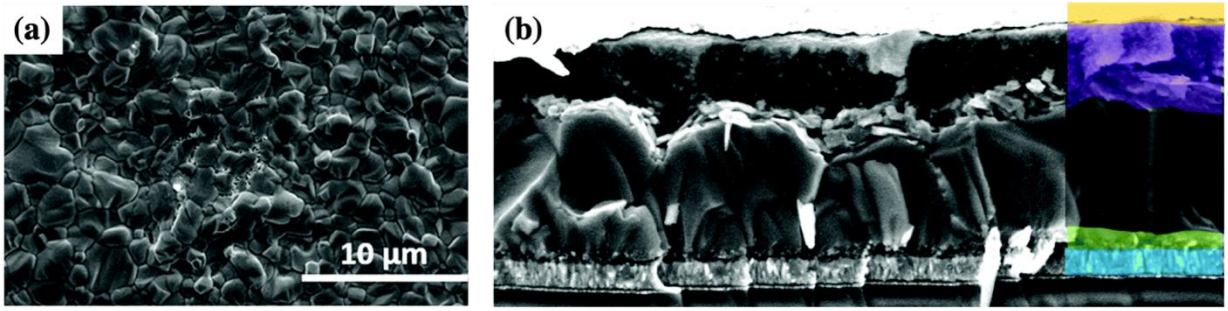

Figure 14. (a) Planar SEM image of $MAPbI_3$ film deposited *via* AACVD. (b) Cross-sectional SEM of completed device. Reproduced from ref. 93 with permission from the Royal Society of Chemistry. Licensed under a Creative Commons Attribution-NonCommercial 3.0 International License (https://creativecommons.org/licenses/by-nc/3.0/).

CONCLUSION AND OUTLOOK

In this review, an overview was presented discussing many reported works regarding the synthesis methods of perovskites and related films based on CVD. Various CVD methods including HCVD, LPCVD and AACVD were classified and summarized. A summary of all identified chemical vapor deposition reports of PSCs is provided in Table 1. Numerous high-quality thin films of perovskites and their derivatives have been deposited successfully, and relative PV devices were fabricated as well. Through CVD, PCEs up to 18.9% of PSCs could be achieved. Furthermore, perovskite solar modules with the active area of 91.8 cm^2 were built up. The significant stability of perovskite films and devices was shown in many reports at the same time. These results proved the versatility and scalability of CVD methods in the perovskite field. In addition, some work also investigated the influence of various deposition parameters, such as temperature, pressure, the kind of carrier gas, flow rate and reaction time, on the morphologies and optoelectrical properties of films, which demonstrated the controllability of the CVD process. The device performance is possible to be improved further through optimizing these parameters.

However, until now, compared with solution-based routes, vapor-based methods are still not widely used to synthesize high-quality perovskite thin films. The highest PCE of a PSC based on CVD-grown perovskite films (18.9%) is still lower than that of the state-of-the-art PSC (25.6%). There are numerous parameters influencing the properties of deposited films in CVD, such as temperatures, carrier flow rate and pressure, which increases the complexity of controlling

chemical and physical reactions in the vapor phase. Unfortunately, the understanding of film growth kinetics in CVD processes is still lacking in detail. Moreover, achieving precision control of the sublimation of organic precursors is challenging in CVD due to their high vapor pressure. The difficulty in controlling the stoichiometry of deposited films also limits the development of CVD-grown films that have complicated compositions and may show better performance. Most reported work on PSCs with high efficiencies based on perovskite films deposited *via* CVD employed multi-step CVD, which increases the cost of the fabrication process and limits the scalability. Although AACVD was adopted as a solution-based CVD to avoid the restriction of precursors, pinholes and excessive thickness of the deposited films make AACVD grown perovskites difficult to utilize in PV applications without further development.

From all works listed in this article, it can be seen that the combination of diverse CVD with other film deposition methods including spin-coating and thermal evaporation is popular, and normally the quality of films could be improved compared with films deposited by a single method. It offers a direction for the further development of CVD, but also puts forward a higher requirement on the understanding of the solid-vapor phase reaction mechanism in the CVD process.

Although some lead-free materials were mentioned, most reports still focused on lead-based perovskites. Considering the toxic and instable nature of lead halide perovskite, further investigation of lead-free or mixed materials in CVD processes would be of interest, which would be beneficial to increase the PSCs' potential of mass production.

Table 1. The summary of identified PSCs fabricated *via* CVD techniques.

Film fabrication method	Steps	Material	Highest PCE (%)	Active area (cm^2)	Ref.
HCVD (thermal evaporation/CVD)	2	$MAPbI_3$	11.8	0.07 – 0.1	19
	2	$FAPbI_3$	14.2	1	21
	2	$MAPbI_3$	15.6	0.09	27
		$FAPbI_3$	9.5	8.8	
			9	12	
	2	$MASn_xPb_{1-x}I_3$	14.04	0.1	28
	2	$Cs_{0.1}FA_{0.9}PbI_{2.9}Br_{0.1}$	9.3	91.8	29
	2	$Cs_{0.1}FA_{0.9}PbI_3$	12.3	22.4	35
HCVD (RUS /CVD)	2	$FAPbI_xBr_{3-x}$	14.7	12	46
HCVD (spin-coating/CVD)	2	$MAPbI_3$	18.9	0.11	23
	2	$MAPbI_3$	17.6	0.06	40
	3	$Cs_{0.07}FA_{0.93}PbI_3$	14.6	12	31
	2	$CsPbBr_3$	5.38	0.12 – 0.15	44
	2	$MAPbI_3$	12.9	0.326	42
Conventional LPCVD	2	$MAPbI_3$	12.73	0.12	22
	2	$MAPbI_3$	6.22	8.4	48
	2	$Cs_xFA_{1-x}PbI_{3-y}Br_y$	17.29 12.24	0.16 41.25	32
	2	$MAPbI_3$	11.7	0.05	51
	3	Cl-doped $MAPbI_3$	10.87	0.0512	54
	2	$MA_3Bi_2I_9$	0.047	–	56
Modified LPCVD (HPCVD)	2	$MAPbI_3$	14.7	0.09	58
	2	$MAPbI_3$	15.15	0.12	65
	3	$MAPbI_3$	13.76	0.12	64
	2	$MAPbI_3$	14.2	–	61
	2	$MAPbI_3$	15.5	–	62
	3	CsBr-doped $FAPbI_3$	18.22	0.09	59
Modified LPCVD (ITCVD)	2	$MAPbI_3$	12.2	0.12	66
	2	$MAPbI_3$	13.33	0.12	67
	2	$MAPbI_3$	11.6	–	68
	2	$MAPbI_3$	16.2	0.01	69
			13.8	1	
CVD	1	$MAPbI_{3-x}Cl_x$	11.1	–	70
	1	$MA_3Bi_2I_9$	0.02	–	75

AACVD	2	$MAPbI_3$	5.42	0.45	[93]

AUTHOR INFORMATION

Corresponding Author

*E-mail: c.j.carmalt@ucl.ac.uk

ORCID

Mingyue Wang: 0000-0003-3084-7619

Claire J. Carmalt: 0000-0003-1788-6971

Author Contributions

The manuscript was written through contributions of all authors. All authors have given approval to the final version of the manuscript.

ACKNOWLEDGMENT

The authors received funding from the Engineering and Physical Sciences Research Council (EPSRC) (grant EP/R511638/1). M. W. would like to thank University College London and China Scholarship Council for the joint Ph.D. scholarship.

REFERENCE

(1) Kojima, A.; Teshima, K.; Shirai, Y.; Miyasaka, T. Organometal Halide Perovskites as Visible-Light Sensitizers for Photovoltaic Cells. *J. Am. Chem. Soc.* **2009**, *131* (17), 6050–6051.

(2) Jeong, J.; Kim, M.; Seo, J.; Lu, H.; Ahlawat, P.; Mishra, A.; Yang, Y.; Hope, M. A.; Eickemeyer, F. T.; Kim, M.; Yoon, Y. J.; Choi, I. W.; Darwich, B. P.; Choi, S. J.; Jo, Y.; Lee, J. H.; Walker, B.; Zakeeruddin, S. M.; Emsley, L.; Rothlisberger, U.; Hagfeldt, A.; Kim, D. S.;

Grätzel, M.; Kim, J. Y. Pseudo-Halide Anion Engineering for α-FAPbI3 Perovskite Solar Cells. *Nature* **2021**, *592* (7854), 381–385.

(3) Burschka, J.; Pellet, N.; Moon, S. J.; Humphry-Baker, R.; Gao, P.; Nazeeruddin, M. K.; Grätzel, M. Sequential Deposition as a Route to High-Performance Perovskite-Sensitized Solar Cells. *Nature* **2013**, *499* (7458), 316–319.

(4) Eperon, G. E.; Burlakov, V. M.; Docampo, P.; Goriely, A.; Snaith, H. J. Morphological Control for High Performance, Solution-Processed Planar Heterojunction Perovskite Solar Cells. *Adv. Funct. Mater.* **2014**, *24* (1), 151–157.

(5) Liu, D.; Kelly, T. L. Perovskite Solar Cells with a Planar Heterojunction Structure Prepared Using Room-Temperature Solution Processing Techniques. *Nat. Photonics* **2014**, *8* (2), 133–138.

(6) Barrows, A. T.; Pearson, A. J.; Kwak, C. K.; Dunbar, A. D. F.; Buckley, A. R.; Lidzey, D. G. Efficient Planar Heterojunction Mixed-Halide Perovskite Solar Cells Deposited via Spray-Deposition. *Energy Environ. Sci.* **2014**, *7* (9), 2944–2950.

(7) Wei, Z.; Chen, H.; Yan, K.; Yang, S. Inkjet Printing and Instant Chemical Transformation of a CH3NH3PbI3/Nanocarbon Electrode and Interface for Planar Perovskite Solar Cells. *Angew. Chemie* **2014**, *126* (48), 13455–13459.

(8) Cotella, G.; Baker, J.; Worsley, D.; De Rossi, F.; Pleydell-Pearce, C.; Carnie, M.; Watson, T. One-Step Deposition by Slot-Die Coating of Mixed Lead Halide Perovskite for Photovoltaic Applications. *Sol. Energy Mater. Sol. Cells* **2017**, *159*, 362–369.

(9) Sutherland, B. R.; Hoogland, S.; Adachi, M. M.; Kanjanaboos, P.; Wong, C. T. O.; McDowell, J. J.; Xu, J.; Voznyy, O.; Ning, Z.; Houtepen, A. J.; Sargent, E. H. Perovskite Thin Films via Atomic Layer Deposition. *Adv. Mater.* **2015**, *27* (1), 53–58.

(10) Liu, M.; Johnston, M. B.; Snaith, H. J. Efficient Planar Heterojunction Perovskite Solar Cells by Vapour Deposition. *Nature* **2013**, *501* (7467), 395–398.

(11) Longo, G.; Gil-Escrig, L.; Degen, M. J.; Sessolo, M.; Bolink, H. J. Perovskite Solar Cells Prepared by Flash Evaporation. *Chem. Commun.* **2015**, *51* (34), 7376–7378.

(12) Shalan, A. E. Challenges and Approaches towards Upscaling the Assembly of Hybrid Perovskite Solar Cells. *Mater. Adv.* **2020**, *1* (3), 292–309.

(13) Swartwout, R.; Hoerantner, M. T.; Bulović, V. Scalable Deposition Methods for Large-Area Production of Perovskite Thin Films. *Energy and Environmental Materials*. 2019, 119–145.

(14) Abegunde, O. O.; Akinlabi, E. T.; Oladijo, O. P.; Akinlabi, S.; Ude, A. U. Overview of Thin Film Deposition Techniques. *AIMS Materials Science*. 2019, 174–199.

(15) Hersee, S. D.; Duchemin, J. P. LOW-PRESSURE CHEMICAL VAPOR DEPOSITION. In *Annual Review of Materials Science*; Annual Reviews 4139 El Camino Way, P.O. Box 10139, Palo Alto, CA 94303-0139, USA, 1982; Vol. 12, 65–80.

(16) Thompson, A. G. MOCVD Technology for Semiconductors. *Mater. Lett.* **1997**, *30* (4), 255–263.

(17) Marchand, P.; Hassan, I. A.; Parkin, I. P.; Carmalt, C. J. Aerosol-Assisted Delivery of Precursors for Chemical Vapour Deposition: Expanding the Scope of CVD for Materials Fabrication. *Dalt. Trans.* **2013**, *42* (26), 9406–9422.

(18) Ha, S. T.; Liu, X.; Zhang, Q.; Giovanni, D.; Sum, T. C.; Xiong, Q. Synthesis of Organic-Inorganic Lead Halide Perovskite Nanoplatelets: Towards High-Performance Perovskite Solar Cells and Optoelectronic Devices. *Adv. Opt. Mater.* **2014**, *2* (9), 838–844.

(19) Leyden, M. R.; Ono, L. K.; Raga, S. R.; Kato, Y.; Wang, S.; Qi, Y. High Performance Perovskite Solar Cells by Hybrid Chemical Vapor Deposition. *J. Mater. Chem. A* **2014**, *2* (44), 18742–18745.

(20) Lewis, D. J.; O'brien, P. Ambient Pressure Aerosol-Assisted Chemical Vapour Deposition of (CH3NH3)PbBr3, an Inorganic-Organic Perovskite Important in Photovoltaics. *Chem. Commun.* **2014**, *50* (48), 6319–6321.

(21) Leyden, M. R.; Lee, M. V; Raga, S. R.; Qi, Y. Large Formamidinium Lead Trihalide Perovskite Solar Cells Using Chemical Vapor Deposition with High Reproducibility and Tunable Chlorine Concentrations. *J. Mater. Chem. A* **2015**, *3* (31), 16097–16103.

(22) Luo, P.; Liu, Z.; Xia, W.; Yuan, C.; Cheng, J.; Lu, Y. Uniform, Stable, and Efficient Planar-Heterojunction Perovskite Solar Cells by Facile Low-Pressure Chemical Vapor Deposition under Fully Open-Air Conditions. *ACS Appl. Mater. Interfaces* **2015**, *7* (4), 2708–2714.

(23) Yin, J.; Qu, H.; Cao, J.; Tai, H.; Li, J.; Zheng, N. Vapor-Assisted Crystallization Control toward High Performance Perovskite Photovoltaics with over 18% Efficiency in the Ambient Atmosphere. *J. Mater. Chem. A* **2016**, *4* (34), 13203–13210.

(24) Luo, P.; Zhou, S.; Xia, W.; Cheng, J.; Xu, C.; Lu, Y. Chemical Vapor Deposition of Perovskites for Photovoltaic Application. *Advanced Materials Interfaces*. 2017.

(25) Jena, A. K.; Kulkarni, A.; Miyasaka, T. Halide Perovskite Photovoltaics : Background , Status , and Future Prospects. *Chem. Rev.* **2019**, *119*, 3036–3103.

(26) Qiu, L.; He, S.; Ono, L. K.; Liu, S.; Qi, Y. Scalable Fabrication of Metal Halide Perovskite Solar Cells and Modules. *ACS Energy Letters*. 2019, 2147–2167.

(27) Leyden, M. R.; Jiang, Y.; Qi, Y. Chemical Vapor Deposition Grown Formamidinium Perovskite Solar Modules with High Steady State Power and Thermal Stability. *J. Mater. Chem. A* **2016**, *4* (34), 13125–13132.

(28) Tavakoli, M. M.; Zakeeruddin, S. M.; Grätzel, M.; Fan, Z. Large-Grain Tin-Rich Perovskite Films for Efficient Solar Cells via Metal Alloying Technique. *Adv. Mater.* **2018**, *30* (11), 1705998.

(29) Qiu, L.; He, S.; Jiang, Y.; Son, D. Y.; Ono, L. K.; Liu, Z.; Kim, T.; Bouloumis, T.; Kazaoui, S.; Qi, Y. Hybrid Chemical Vapor Deposition Enables Scalable and Stable Cs-FA Mixed Cation Perovskite Solar Modules with a Designated Area of 91.8 Cm2 Approaching 10% Efficiency. *J. Mater. Chem. A* **2019**, *7* (12), 6920–6929.

(30) Di Giacomo, F.; Shanmugam, S.; Fledderus, H.; Bruijnaers, B. J.; Verhees, W. J. H.; Dorenkamper, M. S.; Veenstra, S. C.; Qiu, W.; Gehlhaar, R.; Merckx, T.; Aernouts, T.;

Andriessen, R.; Galagan, Y. Up-Scalable Sheet-to-Sheet Production of High Efficiency Perovskite Module and Solar Cells on 6-in. Substrate Using Slot Die Coating. *Sol. Energy Mater. Sol. Cells* **2018**, *181*, 53–59.

(31) Jiang, Y.; Leyden, M. R.; Qiu, L.; Wang, S.; Ono, L. K.; Wu, Z.; Juarez-Perez, E. J.; Qi, Y. Combination of Hybrid CVD and Cation Exchange for Upscaling Cs-Substituted Mixed Cation Perovskite Solar Cells with High Efficiency and Stability. *Adv. Funct. Mater.* **2018**, *28* (1).

(32) Luo, L.; Zhang, Y.; Chai, N.; Deng, X.; Zhong, J.; Huang, F.; Peng, Y.; Ku, Z.; Cheng, Y. B. Large-Area Perovskite Solar Cells with CsxFA1−xPbI3−yBry Thin Films Deposited by a Vapor-Solid Reaction Method. *J. Mater. Chem. A* **2018**, *6* (42), 21143–21148.

(33) Sahli, F.; Miaz, N.; Salsi, N.; Bucher, C.; Schafflützel, A.; Guesnay, Q.; Duchêne, L.; Niesen, B.; Ballif, C.; Jeangros, Q. Vapor Transport Deposition of Methylammonium Iodide for Perovskite Solar Cells. *ACS Appl. Energy Mater.* **2021**, *4* (5), 4333–4343.

(34) Sahli, F.; Miaz, N.; Salsi, N.; Bucher, C.; Schafflützel, A.; Guesnay, Q.; Duchêne, L.; Niesen, B.; Ballif, C.; Jeangros, Q. Vapor Transport Deposition of Methylammonium Iodide for Perovskite Solar Cells. *ACS Appl. Energy Mater.* **2021**, *4* (5), 4333–4343.

(35) Qiu, L.; He, S.; Liu, Z.; Ono, L. K.; Son, D. Y.; Liu, Y.; Tong, G.; Qi, Y. Rapid Hybrid Chemical Vapor Deposition for Efficient and Hysteresis-Free Perovskite Solar Modules with an Operation Lifetime Exceeding 800 Hours. *J. Mater. Chem. A* **2020**, *8* (44), 23404–23412.

(36) Momblona, C.; Gil-Escrig, L.; Bandiello, E.; Hutter, E. M.; Sessolo, M.; Lederer, K.; Blochwitz-Nimoth, J.; Bolink, H. J. Efficient Vacuum Deposited P-i-n and n-i-p Perovskite Solar

Cells Employing Doped Charge Transport Layers. *Energy Environ. Sci.* **2016**, *9* (11), 3456–3463.

(37) Vaynzof, Y. The Future of Perovskite Photovoltaics—Thermal Evaporation or Solution Processing? *Adv. Energy Mater.* **2020**, *10* (48).

(38) Liu, P.; Chen, Y.; Xiang, H.; Yang, X.; Wang, W.; Ran, R.; Zhou, W.; Shao, Z. Benefitting from Synergistic Effect of Anion and Cation in Antimony Acetate for Stable CH3NH3PbI3-Based Perovskite Solar Cell with Efficiency Beyond 21%. *Small* **2021**.

(39) Stümmler, D.; Sanders, S.; Mühlenbruch, S.; Pfeiffer, P.; Simkus, G.; Heuken, M.; Vescan, A.; Kalisch, H. Fabrication of Methylammonium Bismuth Iodide Layers Employing Methylamine Vapor Exposure. *Phys. Status Solidi Appl. Mater. Sci.* **2019**, *216* (18).

(40) Ng, A.; Ren, Z.; Shen, Q.; Cheung, S. H.; Gokkaya, H. C.; So, S. K.; Djurišić, A. B.; Wan, Y.; Wu, X.; Surya, C. Crystal Engineering for Low Defect Density and High Efficiency Hybrid Chemical Vapor Deposition Grown Perovskite Solar Cells. *ACS Appl. Mater. Interfaces* **2016**, *8* (48), 32805–32814.

(41) Shen, Q.; Ng, A.; Ren, Z.; Gokkaya, H. C.; Djurišić, A. B.; Zapien, J. A.; Surya, C. Characterization of Low-Frequency Excess Noise in CH3NH3PbI3-Based Solar Cells Grown by Solution and Hybrid Chemical Vapor Deposition Techniques. *ACS Appl. Mater. Interfaces* **2018**, *10* (1), 371–380.

(42) Mortan, C.; Hellmann, T.; Buchhorn, M.; d'Eril Melzi, M.; Clemens, O.; Mayer, T.; Jaegermann, W. Preparation of Methylammonium Lead Iodide (CH3NH3PbI3) Thin Film

Perovskite Solar Cells by Chemical Vapor Deposition Using Methylamine Gas (CH3NH2) and Hydrogen Iodide Gas. *Energy Sci. Eng.* **2020**, *8* (9), 3165–3173.

(43) Zhou, Z.; Wang, Z.; Zhou, Y.; Pang, S.; Wang, D.; Xu, H.; Liu, Z.; Padture, N. P.; Cui, G. Methylamine-Gas-Induced Defect-Healing Behavior of CH 3 NH 3 PbI 3 Thin Films for Perovskite Solar Cells. *Angew. Chemie* **2015**, *127* (33), 9841–9845.

(44) Luo, P.; Zhou, Y.; Zhou, S.; Lu, Y.; Xu, C.; Xia, W.; Sun, L. Fast Anion-Exchange from CsPbI3 to CsPbBr3 via Br2-Vapor-Assisted Deposition for Air-Stable All-Inorganic Perovskite Solar Cells. *Chem. Eng. J.* **2018**, *343* (March), 146–154.

(45) Luo, P.; Zhou, Y.; Xia, W.; Zhou, S.; Liu, J.; Lu, Y.; Xu, C.; Sun, L. Colorful, Bandgap-Tunable, and Air-Stable CsPb(IxBr1-x)3 Inorganic Perovskite Films via a Novel Sequential Chemical Vapor Deposition. *Ceram. Int.* **2018**, *44* (11), 12783–12788.

(46) Jiang, Y.; Remeika, M.; Hu, Z.; Juarez-Perez, E. J.; Qiu, L.; Liu, Z.; Kim, T.; Ono, L. K.; Son, D. Y.; Hawash, Z.; Leyden, M. R.; Wu, Z.; Meng, L.; Hu, J.; Qi, Y. Negligible-Pb-Waste and Upscalable Perovskite Deposition Technology for High-Operational-Stability Perovskite Solar Modules. *Adv. Energy Mater.* **2019**, *9* (13).

(47) Jensen, K. F.; Graves, D. B. Modeling and Analysis of Low Pressure CVD Reactors. *J. Electrochem. Soc.* **1983**, *130* (9), 1950–1957.

(48) Shen, P. S.; Chen, J. S.; Chiang, Y. H.; Li, M. H.; Guo, T. F.; Chen, P. Low-Pressure Hybrid Chemical Vapor Growth for Efficient Perovskite Solar Cells and Large-Area Module. *Adv. Mater. Interfaces* **2016**, *3* (8).

(49) Kim, J.; Kim, H. P.; Teridi, M. A. M.; Yusoff, A. R. B. M.; Jang, J. Bandgap Tuning of Mixed Organic Cation Utilizing Chemical Vapor Deposition Process. *Sci. Rep.* **2016**, *6*.

(50) Chen, Y.; Yang, J.; Wang, S.; Wu, Y.; Yuan, N.; Zhang, W. H. Interfacial Contact Passivation for Efficient and Stable Cesium-Formamidinium Double-Cation Lead Halide Perovskite Solar Cells. *iScience* **2020**, *23* (1).

(51) Ngqoloda, S.; Arendse, C. J.; Muller, T. F.; Miceli, P. F.; Guha, S.; Mostert, L.; Oliphant, C. J. Air-Stable Hybrid Perovskite Solar Cell by Sequential Vapor Deposition in a Single Reactor. *ACS Appl. Energy Mater.* **2020**, *3* (3), 2350–2359.

(52) Magubane, S. S.; Arendse, C. J.; Ngqoloda, S.; Cummings, F.; Mtshali, C.; Bolokang, A. S. Chemical Vapor Deposited Mixed Metal Halide Perovskite Thin Films. *Materials (Basel).* **2021**, *14* (13), 3526.

(53) Burns, R.; Ngqoloda, S.; Arendse, C. J.; Lavina, B.; Dahal, A.; Singh, D. K.; Guha, S. Probing Structure–Property Relationship in Chemical Vapor Deposited Hybrid Perovskites by Pressure and Temperature. *J. Mater. Res.* **2021**, *36* (9), 1805–1812.

(54) Ngqoloda, S.; Arendse, C. J.; Guha, S.; Muller, T. F.; Klue, S. C.; Magubane, S. S.; Oliphant, C. J. Mixed-Halide Perovskites Solar Cells through PbICl and PbCl2 Precursor Films by Sequential Chemical Vapor Deposition. *Sol. Energy* **2021**, *215* (November 2020), 179–188.

(55) Hoat, P. D.; Ha, H.-H.; Hung, P. T.; Hien, V. X.; Lee, S.; Lee, J.-H.; Heo, Y.-W. Synthesis of Cs2SnI6 Perovskite Thin Film by Low-Pressure Chemical Vapor Deposition Method. *Thin Solid Films* **2021**, *732* (June), 138799.

(56) Stümmler, D.; Sanders, S.; Gerstenberger, F.; Pfeiffer, P.; Simkus, G.; Baumann, P. K.; Heuken, M.; Vescan, A.; Kalisch, H. Reaction Engineering of CVD Methylammonium Bismuth Iodide Layers for Photovoltaic Applications. *J. Mater. Res.* **2019**, *34* (4), 608–615.

(57) Ishteev, A.; Luchnikov, L.; Muratov, D. S.; Voronova, M.; Forde, A.; Inerbaev, T.; Vanyushin, V.; Saranin, D.; Yusupov, K.; Kuznetsov, D.; Di Carlo, A. Single Source Chemical Vapor Deposition (SsCVD) for Highly Luminescent Inorganic Halide Perovskite Films. *Appl. Phys. Lett.* **2021**, *119* (7).

(58) Peng, Y.; Jing, G.; Cui, T. A Hybrid Physical-Chemical Deposition Process at Ultra-Low Temperatures for High-Performance Perovskite Solar Cells. *J. Mater. Chem. A* **2015**, *3* (23), 12436–12442.

(59) Tong, G.; Li, H.; Li, G.; Zhang, T.; Li, C.; Yu, L.; Xu, J.; Jiang, Y.; Shi, Y.; Chen, K. Mixed Cation Perovskite Solar Cells by Stack-Sequence Chemical Vapor Deposition with Self-Passivation and Gradient Absorption Layer. *Nano Energy* **2018**, *48* (March), 536–542.

(60) Yang, C.; Shan, X.; Xie, T. Hysteresis Passivation in Planar Perovskite Solar Cells Utilizing Facile Chemical Vapor Deposition Process and PCBM Interlayer. *Energies* **2019**, *12* (23).

(61) Peng, Y.; Jing, G.; Cui, T. High-Performance Perovskite Solar Cells Fabricated by Vapor Deposition with Optimized PbI2 Precursor Films. *RSC Adv.* **2015**, *5* (116), 95847–95853.

(62) Wei, X.; Peng, Y.; Jing, G.; Cui, T. Planar Structured Perovskite Solar Cells by Hybrid Physical Chemical Vapor Deposition with Optimized Perovskite Film Thickness. *Jpn. J. Appl. Phys.* **2018**, *57* (5), 052301.

(63) Wu, Y.; Islam, A.; Yang, X.; Qin, C.; Liu, J.; Zhang, K.; Peng, W.; Han, L. Retarding the Crystallization of PbI2 for Highly Reproducible Planar-Structured Perovskite Solar Cells via Sequential Deposition. *Energy Environ. Sci.* **2014**, *7* (9), 2934–2938.

(64) Luo, P.; Liu, Z.; Xia, W.; Yuan, C.; Cheng, J.; Xu, C.; Lu, Y. Chlorine-Conducted Defect Repairment and Seed Crystal-Mediated Vapor Growth Process for Controllable Preparation of Efficient and Stable Perovskite Solar Cells. *J. Mater. Chem. A* **2015**, *3* (45), 22949–22959.

(65) Wang, B.; Chen, T. Exceptionally Stable CH3 NH3 Pbi3 Films in Moderate Humid Environmental Condition. *Adv. Sci.* **2015**, *3* (2).

(66) Luo, P.; Liu, Z.; Xia, W.; Yuan, C.; Cheng, J.; Lu, Y. A Simple in Situ Tubular Chemical Vapor Deposition Processing of Large-Scale Efficient Perovskite Solar Cells and the Research on Their Novel Roll-over Phenomenon in J-V Curves. *J. Mater. Chem. A* **2015**, *3* (23), 12443–12451.

(67) Liu, Z.; Luo, P.; Xia, W.; Zhou, S.; Cheng, J.; Sun, L.; Xu, C.; Lu, Y. Acceleration Effect of Chlorine in the Gas-Phase Growth Process of CH3NH3PbI3(Cl) Films for Efficient Perovskite Solar Cells. *J. Mater. Chem. C* **2016**, *4* (26), 6336–6344.

(68) Ioakeimidis, A.; Christodoulou, C.; Lux-Steiner, M.; Fostiropoulos, K. Effect of PbI2 Deposition Rate on Two-Step PVD/CVD All-Vacuum Prepared Perovskite. *J. Solid State Chem.* **2016**, *244*, 20–24.

(69) Li, G.; Ho, J. Y. L.; Wong, M.; Kwok, H. S. Low Cost, High Throughput and Centimeter-Scale Fabrication of Efficient Hybrid Perovskite Solar Cells by Closed Space Vapor Transport. *Phys. Status Solidi - Rapid Res. Lett.* **2016**, *10* (2), 153–157.

(70) Tavakoli, M. M.; Gu, L.; Gao, Y.; Reckmeier, C.; He, J.; Rogach, A. L.; Yao, Y.; Fan, Z. Fabrication of Efficient Planar Perovskite Solar Cells Using a One-Step Chemical Vapor Deposition Method. *Sci. Rep.* **2015**, *5* (1), 14083.

(71) Tran, V. D.; Pammi, S. V. N.; Dao, V. D.; Choi, H. S.; Yoon, S. G. Chemical Vapor Deposition in Fabrication of Robust and Highly Efficient Perovskite Solar Cells Based on Single-Walled Carbon Nanotubes Counter Electrodes. *J. Alloys Compd.* **2018**, *747*, 703–711.

(72) Pammi, S. V. N.; Lee, H. W.; Eom, J. H.; Yoon, S. G. Predominant Stable MAPbI3 Films Deposited via Chemical Vapor Deposition: Stability Studies in Illuminated and Darkened States Coupled with Temperature under an Open-Air Atmosphere. *ACS Appl. Energy Mater.* **2018**, *1* (7), 3301–3312.

(73) Ishteev, A.; Luchnikov, L.; Muratov, D. S.; Voronova, M.; Forde, A.; Inerbaev, T.; Vanyushin, V.; Saranin, D.; Yusupov, K.; Kuznetsov, D.; Di Carlo, A. Single Source Chemical Vapor Deposition (SsCVD) for Highly Luminescent Inorganic Halide Perovskite Films. *Appl. Phys. Lett.* **2021**, *119* (7).

(74) Chen, X.; Myung, Y.; Thind, A.; Gao, Z.; Yin, B.; Shen, M.; Cho, S. B.; Cheng, P.; Sadtler, B.; Mishra, R.; Banerjee, P. Atmospheric Pressure Chemical Vapor Deposition of Methylammonium Bismuth Iodide Thin Films. *J. Mater. Chem. A* **2017**, *5* (47), 24728–24739.

(75) Sanders, S.; Stümmler, D.; Pfeiffer, P.; Ackermann, N.; Simkus, G.; Heuken, M.; Baumann, P. K.; Vescan, A.; Kalisch, H. Chemical Vapor Deposition of Organic-Inorganic Bismuth-Based Perovskite Films for Solar Cell Application. *Sci. Rep.* **2019**, *9* (1).

(76) Zhou, Y.; Fernando, K.; Wan, J.; Liu, F.; Shrestha, S.; Tisdale, J.; Sheehan, C. J.; Jones, A. C.; Tretiak, S.; Tsai, H.; Huang, H.; Nie, W. Millimeter-Size All-Inorganic Perovskite Crystalline Thin Film Grown by Chemical Vapor Deposition. *Adv. Funct. Mater.* **2021**, *31* (23).

(77) Bhachu, D. S.; Sathasivam, S.; Sankar, G.; Scanlon, D. O.; Cibin, G.; Carmalt, C. J.; Parkin, I. P.; Watson, G. W.; Bawaked, S. M.; Obaid, A. Y.; Al-Thabaiti, S.; Basahel, S. N. Solution Processing Route to Multifunctional Titania Thin Films: Highly Conductive and Photcatalytically Active Nb:TiO2. *Adv. Funct. Mater.* **2014**, *24* (32), 5075–5085.

(78) Crick, C. R.; Ismail, S.; Pratten, J.; Parkin, I. P. An Investigation into Bacterial Attachment to an Elastomeric Superhydrophobic Surface Prepared via Aerosol Assisted Deposition. *Thin Solid Films* **2011**, *519* (11), 3722–3727.

(79) Bhachu, D. S.; Scanlon, D. O.; Saban, E. J.; Bronstein, H.; Parkin, I. P.; Carmalt, C. J.; Palgrave, R. G. Scalable Route to CH3NH3PbI3 Perovskite Thin Films by Aerosol Assisted Chemical Vapour Deposition. *J. Mater. Chem. A* **2015**, *3* (17), 9071–9073.

(80) Ke, J. C.-R.; Lewis, D. J.; Walton, A. S.; Spencer, B. F.; O'Brien, P.; Thomas, A. G.; Flavell, W. R. Ambient-Air-Stable Inorganic Cs2SnI6 Double Perovskite Thin Films via Aerosol-Assisted Chemical Vapour Deposition. *J. Mater. Chem. A* **2018**, *6* (24), 11205–11214.

(81) Alharbi, Y. T.; Alam, F.; Parvez, K.; Missous, M.; Lewis, D. J. Molecular Precursor Route to Bournonite (CuPbSbS3) Thin Films and Powders. *Inorg. Chem.* **2021**, *60* (17), 13691–13698.

(82) Wang, M.; Sanchez-Perez, C.; Habib, F.; Blunt, M. O.; Carmalt, C. J. Scalable Production of Ambient Stable Hybrid Bismuth-Based Materials: AACVD of Phenethylammonium Bismuth Iodide Films**. *Chem. - A Eur. J.* **2021**, *27* (36), 9406–9413.

(83) Knapp, C. E.; Carmalt, C. J. Solution Based CVD of Main Group Materials. *Chemical Society Reviews*. Royal Society of Chemistry 2016, 1036–1064.

(84) Afzaal, M.; Yates, H. M. Growth Patterns and Properties of Aerosol-Assisted Chemical Vapor Deposition of CH3NH3PbI3 Films in a Single Step. *Surface and Coatings Technology*. 2017, 336–340.

(85) Alam, F.; Lewis, D. J. Thin Films of Formamidinium Lead Iodide (FAPI) Deposited Using Aerosol Assisted Chemical Vapour Deposition (AACVD). *Sci. Rep.* **2020**, *10* (1), 1–7.

(86) Daskalakis, S.; Wang, M.; Carmalt, C. J.; Vernardou, D. Electrochemical Investigation of Phenethylammonium Bismuth Iodide as Anode in Aqueous Zn2+ Electrolytes. *Nanomaterials* **2021**, *11* (3), 1–8.

(87) Nishinaka, H.; Yoshimoto, M. Solution-Based Mist CVD Technique for CH 3 NH 3 Pb(Br 1-x Cl x) 3 Inorganic-Organic Perovskites. *Jpn. J. Appl. Phys.* **2016**, *55* (10), 100308.

(88) Aamir, M.; Sher, M.; Khan, M. D.; Malik, M. A.; Akhtar, J.; Revaprasadu, N. Controlled Synthesis of All Inorganic CsPbBr2I Perovskite by Non-Template and Aerosol Assisted Chemical Vapour Deposition. *Mater. Lett.* **2017**, *190*, 244–247.

(89) Basak, S.; Afzaal, M.; Yates, H. M. Optically Tuned and Large-Grained Bromine Doped CH3NH3PbI3 Perovskite Thin Films via Aerosol-Assisted Chemical Vapour Deposition. *Mater. Chem. Phys.* **2019**, *223*, 157–163.

(90) Ke, C. R.; Lewis, D. J.; Walton, A. S.; Chen, Q.; Spencer, B. F.; Mokhtar, M. Z.; Compean-Gonzalez, C. L.; O'Brien, P.; Thomas, A. G.; Flavell, W. R. Air-Stable Methylammonium Lead Iodide Perovskite Thin Films Fabricated via Aerosol-Assisted Chemical Vapor Deposition from a Pseudohalide Pb(SCN)2 Precursor. *ACS Appl. Energy Mater.* **2019**, *2* (8), 6012–6022.

(91) Chen, S.; Briscoe, J.; Shi, Y.; Chen, K.; Wilson, R. M.; Dunn, S.; Binions, R. A Simple, Low-Cost CVD Route to High-Quality CH3NH3PbI3 Perovskite Thin Films. *CrystEngComm* **2015**, *17* (39), 7486–7489.

(92) Afzaal, M.; Salhi, B.; Al-Ahmed, A.; Yates, H. M.; Hakeem, A. S. Surface-Related Properties of Perovskite CH3NH3PbI3 Thin Films by Aerosol-Assisted Chemical Vapour Deposition. *J. Mater. Chem. C* **2017**, *5* (33), 8366–8370.

(93) Ratnasingham, S. R.; Mohan, L.; Daboczi, M.; Degousée, T.; Binions, R.; Fenwick, O.; Kim, J.-S.; McLachlan, M.; Briscoe, J. Novel Scalable Aerosol-Assisted CVD Route for Perovskite Solar Cells. *Mater. Adv.* **2021**, 1606–1612.

(94) Du, T.; Ratnasingham, S. R.; Kosasih, F. U.; Macdonald, T. J.; Mohan, L.; Augurio, A.; Ahli, H.; Lin, C. T.; Xu, S.; Xu, W.; Binions, R.; Ducati, C.; Durrant, J. R.; Briscoe, J.; McLachlan, M. A. Aerosol Assisted Solvent Treatment: A Universal Method for Performance and Stability Enhancements in Perovskite Solar Cells. *Adv. Energy Mater.* **2021**, *11* (33), 2101420.